GLOBAL JOURNAL
OF MEDICAL RESEARCH - I: SURGERIES & CARDIOVASCULAR SYSTEM

Volume 26 | Issue 1 | 2026 Article ID: GJMR-255059 Language: English

CATALOGING

PACS • 03.50.De, 87.19.Hh MESH • D002318 IEEE • K.3.4 ARXIV • physics.gen-ph

Analysis of the Medical Efficacy and Physical-Chemical Mechanism of Torsion Fields Generated by Scalar Waves in the Treatment of Cardiovascular and Cerebrovascular Diseases

Article Record

Jianzhong Jiang[§ ϑ *]
ϑ PhD
*Corresponding Author

He-yuan LI

Xi-qi CHEN

§ School of Mechanical & Engineering, Jiangnan University; Wuxi, 214122, China

RECEIVED	ACCEPTED	ONLINE PUBLISHED	PUBLISHED	PEER REVIEW
2026-03-21	2026-04-01	2026-06-17	2026-08-17	Double Blind

Abstract

Due to the absence of rigorous mathematical modeling and extensive experimental validation, the applications of torsion fields generated by scalar waves (SWs)—such as superluminality, zero-point energy extraction and enhancement of the human energy field—remain in the hypothetical phase. The mainstream physics community has yet to recognize torsion field as a fundamental force; thus, current researches on the medical functionalities of scalar wave and torsion field still fall within the domain of medical fringe science. Building upon the precise modeling of the vacuum scalar wave equation and particle propagation mode, we derived a theoretical framework for the generation of artificial torsion fields via vortex electromagnetic fields of SWs. We further conducted a detailed analysis of the dynamic characteristics of torsion fields in thrombus removal, as well as the interaction between scalar waves and free electrons carried by erythrocytes. This work reveals two key insights: the medical utility of torsion fields generated by SWs in the treatment of cardiovascular and cerebrovascular diseases; and the essential relationship between vortex electromagnetic fields of SWs and torsion fields. Specifically, the torsion field is the acceleration field of local spatial tangential rotational motion induced by the vortex motion of the scalar wave vortex electromagnetic fields.

Quantum electrodynamics | scalar wave | torsion field | gravitational field | thrombus

AI USE STATEMENT
The authors confirm that no artificial intelligence (AI) tools were used in the writing or analysis of this study. All content is the original work of the authors.

FUNDING
I would like to thank my wife, Ms. Xue Jingwen for her hard family work and support...

CONFLICT OF INTEREST
The authors declare no competing interests.

DATA AVAILABILITY
Data sharing is not applicable to this article as no new data were...

ETHICS
Ethical approval was not required for this study because the research is based solely on...

CONSENT
Not applicable for this article.

TRIAL REG.
Not applicable.

Crossref DOI: 10.34257/GJMRI255059

How to Cite: Jiang et al. (2026). Analysis of the Medical Efficacy and Physical-Chemical Mechanism of Torsion Fields Generated by Scalar Waves in the Treatment of Cardiovascular and Cerebrovascular Diseases. Global Journal of Medical Research, 26(1), 7-14. DOI: 10.34257/GJMRI255059

AR Experience Web Page DOI

Print ISSN 0975-5888

Online ISSN 2249-4618

Under the strict compliance and defined process of

METADATA CONTINUATION

AUTHOR CONTACT QR LEDGER

Jianzhong Jiang§ϑ*

He-yuan LI

Xi-qi CHEN

FULL FUNDING STATEMENT

I would like to thank my wife, Ms. Xue Jingwen for her hard family work and support for my creation of this thesis.

FULL DATA AVAILABILITY STATEMENT

Data sharing is not applicable to this article as no new data were created or analyzed in this study.

FULL ETHICS STATEMENT

Ethical approval was not required for this study because the research is based solely on anonymous, publicly available data and does not involve direct interaction with human participants.

ARCHIVAL RECORD

GJMR · Vol 26 · Issue 1 · 2026

Article ID GJMR-255059 · DOI 10.34257/GJMRI255059

Print ISSN 0975-5888 · Online ISSN 2249-4618

Global Journal of Medical Research - Section I
GJMR Volume 26 Issue 1

Analysis of the Medical Efficacy and Physical-Chemical Mechanism of Torsion Fields Generated by Scalar Waves in the Treatment of Cardiovascular and Cerebrovascular Diseases

Jianzhong Jiang[§ ϑ *], He-yuan LI[§], and Xi-qi CHEN[§]

Affiliations
§ School of Mechanical & Engineering, Jiangnan University; Wuxi, 214122, China

Qualifications / Designations
ϑ PhD

Abstract

Due to the absence of rigorous mathematical modeling and extensive experimental validation, the applications of torsion fields generated by scalar waves (SWs)—such as superluminality, zero-point energy extraction and enhancement of the human energy field—remain in the hypothetical phase. The mainstream physics community has yet to recognize torsion field as a fundamental force; thus, current researches on the medical functionalities of scalar wave and torsion field still fall within the domain of medical fringe science. Building upon the precise modeling of the vacuum scalar wave equation and particle propagation mode, we derived a theoretical framework for the generation of artificial torsion fields via vortex electromagnetic fields of SWs. We further conducted a detailed analysis of the dynamic characteristics of torsion fields in thrombus removal, as well as the interaction between scalar waves and free electrons carried by erythrocytes. This work reveals two key insights: the medical utility of torsion fields generated by SWs in the treatment of cardiovascular and cerebrovascular diseases; and the essential relationship between vortex electromagnetic fields of SWs and torsion fields. Specifically, the torsion field is the acceleration field of local spatial tangential rotational motion induced by the vortex motion of the scalar wave vortex electromagnetic fields.

Keywords: *Quantum electrodynamics, scalar wave, torsion field, gravitational field, thrombus*

* **Corresponding Author**
Jianzhong Jiang

DOI
10.34257/GJMRI255059

1. Introduction

Traditional technologies of transverse electromagnetic field (TEMF) for treating cardiovascular and cerebrovascular diseases primarily focus on the regulatory effects of physical therapies or bioactive substances (e.g., endothelin-1, nitric oxide) on vascular endothelial cells and blood circulation, with underlying mechanisms encompassing techniques such as TEMF stimulation, biofeedback, and microcurrent modulation[1–5]. EMF technology can act on vascular endothelial cells to promote nitric oxide release, thereby facilitating peripheral vasodilation and reducing blood flow resistance. The biofeedback module enables real-time monitoring of users' heart rate variability, balancing sympathetic and parasympathetic neural activities by modulating autonomic nervous function. Microcurrent stimulation can influence local tissue metabolism, accelerate lactic acid clearance, and enhance cell membrane stability.

Typically, the amplitude of electromagnetic longitudinal waves (scalar waves, SWs) is considerably smaller than that of the source transverse electromagnetic waves (TEM waves) generating them[6], thus they are often neglected. However, in certain scenarios—such as the near-field region—existing Maxwell's equations fail to fully characterize their electromagnetic properties, necessitating the consideration of SWs[7,8]. Substantial SWs can be generated when two coherent, out-of-phase TEM waves interfere[9,10]. The vortex electromagnetic field of SWs gives rise to a unique force field known as the torsion field[11–16]. While the static torsion field exhibits extremely weak intensity (approximately 10^{27} times weaker than gravitational force), its dynamic intensity is substantially enhanced[17]. Torsion fields possess properties including superluminal propagation, non-shielding, zero-point vacuum energy extraction, and memory effects [18], and their potential and practical applications in medicine have gained widespread recognition and attention [19–23].

Nevertheless, due to the absence of rigorous wave equations and particle propagation model[24], applied researches of torsion fields generated by SWs on energy medicine has encountered technical bottlenecks, such as optimizing energy intensity and therapeutic frequencies. Consequently, many scholars have questioned the efficacy and reliability of scalar wave and torsion field therapy[25]. Additionally, conventional perspectives maintain that generating pure torsion fields generated by SWs is highly challenging, requiring precise control of the phase difference between two source waves to the picosecond level, stable interference point spatial conditions, and mitigating environmental noise, metal reflections, and geomagnetic disturbances. Even minimal phase drift can cause SWs to collapse into ordinary TEM waves, resulting in the loss of all unique properties.

As a result, current researches on torsion fields generated by SWs remain within the realm of fringe science, and no clear consensus has been established in authoritative medical literature regarding their medical functions and physicochemical mechanisms in treating cardiovascular and cerebrovascular diseases. By constructing

accurate models of the vacuum scalar wave equation and particle propagation, we aim to derive a theoretical framework for torsion fields generated by SWs and elucidate their intrinsic connections to mass and gravitational field. The development of these novel theoretical models may provide new tools and methodological approaches for analyzing the medical efficacy and physicochemical mechanisms of torsion fields generated by SWs in cardiovascular and cerebrovascular disease treatment.

2. The essence of electromagnetic fields

Both torsion field and SW wave are associated with spin effects. The torsion field stems from spacetime distortion [11], whereas SW waves originate from vortex electromagnetic fields [6]. Thus, torsion fields are closely related to SW waves, and investigating torsion fields necessitates a prior clarification of the essence of electromagnetic fields.

From the law of total current [26], the electromagnetic field $\vec{E}/\vec{B}$ in a conductor can be expressed as

$$\begin{aligned}\frac{1}{\mu\varepsilon}\nabla\times\vec{B} &= \frac{\partial\vec{E}}{\partial t}+\frac{\sigma}{\mathcal{E}}\vec{E}=\frac{\partial\vec{E}}{\partial t}+\frac{1}{\mathcal{E}}\vec{J}=\frac{\partial\vec{E}}{\partial t}-\frac{\rho}{\mathcal{E}}\vec{V}_e\\ &=\left(\vec{V}_e\cdot\nabla\right)\vec{E}-\left(\nabla\cdot\vec{E}\right)\vec{V}_e-\left(\vec{E}\cdot\nabla\right)\vec{V}_e+\left(\nabla\cdot\vec{V}_e\right)\vec{E}\\ &=\nabla\times\left(\vec{E}\times\vec{V}_e\right).\end{aligned}\tag{1}$$

Thus, it follows from Eq. (1) that

$$\frac{1}{\mu\varepsilon}\vec{B}=-\vec{V}_e\times\vec{E}.\tag{2}$$

By synthesizing Eqs. (1) and (2), it is evident that the law of total current embodies a fundamental implication of the electromagnetic field: the relativistic effect of the propagation velocity of the electric field through positive charges (holes) in the conductor—specifically, the moving velocity of the electric field, $-\vec{V}_e$—is converted into the magnetic field within the conductor, which aligns with the principle that a moving electric field generates a magnetic field [27].

Employing the same analytical approach, Faraday's Law of Electromagnetic Induction [26] yields that

$$\begin{aligned}\nabla\times\vec{E} &= -\frac{\partial\vec{B}}{\partial t}=\left(\vec{V}_B\cdot\nabla\right)\vec{B}\\ &=-\left(\nabla\cdot\vec{B}\right)\vec{V}_B-\left(\vec{B}\cdot\nabla\right)\vec{V}_B+\left(\nabla\cdot\vec{V}_B\right)\vec{B}+\left(\vec{V}_B\cdot\nabla\right)\vec{B}\\ &=\nabla\times\left(\vec{B}\times\vec{V}_B\right).\end{aligned}\tag{3}$$

Then, according to Eq. (3), we have

$$\vec{E}=-\vec{V}_B\times\vec{B},\tag{4}$$

By synthesizing Eqs. (3) and (4), it is evident that Faraday's law of electromagnetic induction embodies another fundamental implication of the electromagnetic field: the magnetic field within the conductor is converted into an electric field in the conductor via the relativistic effect of the magnetic field's velocity vector $\vec{V}_B$—specifically, a moving magnetic field generates an electric field [28].

In Eq. (4), $\vec{V}_B$ serves as both the wave velocity of electromagnetic transverse waves [26] and the velocity of magnetic field motion [28]. According to the principle of duality, the component $-V_{ez}$ of $-\vec{V}_e$ along the electromagnetic field propagation direction z is not only the velocity at which positive charges propagate the electric field (or the velocity of the electric field itself) [10], but should also correspond to the wave velocity of some form of wave. It is hypothesized that while the TEM waves $\vec{E}_t/\vec{B}_t$ propagate along the z-direction within the conductor, there exists a type of electromagnetic longitudinal waves, i.e. SWs $\vec{E}_z/\vec{B}_\theta$ that propagates along the same z-direction with frequency ω_P and wave velocity V_{ez} [29].

Eq. (4)—which is associated with Faraday's law of electromagnetic induction for the TEM waves $\vec{E}_t/\vec{B}_t$—can be expressed in terms of the electromagnetic scalar potential φ and magnetic vector potential $\vec{A}$ as follows [26]

$$\begin{aligned}\vec{E}_t &= -\nabla\varphi-\frac{\partial\vec{A}_t}{\partial t}\\ &=-\vec{V}_B\times\left(\nabla\times\vec{A}_t\right)\\ &=-j\vec{k}\varphi+j\vec{A}_t\omega\\ &=-j\vec{k}\left(\vec{V}_B\cdot\vec{A}\right)+j\vec{A}_t\left(\vec{k}\cdot\vec{V}_B\right)\\ &=-j\vec{k}\left(\vec{V}_B\cdot\vec{A}\right)+j\vec{A}_t\omega,\end{aligned}$$

which gives that

$$\varphi=\vec{V}_B\cdot\vec{A}=V_BA_z.\tag{5}$$

In accordance with the Lorenz gauge condition applicable to metallic conductors [26], we can obtain

$$\nabla\cdot\vec{A}=-\mu\varepsilon\frac{\partial\varphi}{\partial t}=\mu\varepsilon j\omega_PV_BA_z=\frac{j\omega_PA_z}{V_{ez}}.$$

Thus, it follows that

$$\frac{1}{\mu\varepsilon}=V_{ez}V_B.\tag{6}$$

Eq. (6) reveals a constraint relation between $-\vec{V}_{ez}$ (the propagation velocity of the electric field of TEM waves in the conductor medium, i.e., the wave speed of SW waves) and $\vec{V}_B$ (the velocity of magnetic field motion, i.e., the wave speed of TEM waves): the product of the two quantities does not exceed the square of the speed of light in the conductor. For typical metallic conductors [30], we can obtain that

$$V_{ez}\sim10^{10}\text{ m/s}\gg V_B=\sqrt{\frac{2\omega}{\mu\sigma}}\sim10^6\text{ m/s},\tag{7}$$

which implies that the wave velocity V_{ez} of the SW propagating within the conductor could be superluminal.

3. The particle propagation mode for SWs

When two coherent light waves (termed "source light waves") with identical frequency, equal amplitude, opposite propagation directions, and a phase difference of π are superposed in a vacuum, a pair of vacuum scalar waves $\vec{B}_z/\vec{E}_\theta$ are generated [6]. Upon superposition, the resultant TEM fields $\vec{B}_t/\vec{E}_t$ vanish, creating the illusion of energy disappearance. However, according to the Aharonov-Bohm effect [31], this process merely corresponds to the extinction of the TEM waves—the magnetic vector potential $\vec{A}_\theta$ and electromagnetic scalar potential φ_θ in the vacuum do not cease to exist, but instead transform into the SWs [6].

By analogy with the electromagnetic fields in conductive media, the electromagnetic fields of vacuum SWs $\vec{B}_z/\vec{E}_\theta$ should also satisfy

electromagnetic conversion formulas shown as Eqs. (2) and (4). We thus hypothesize

$$\vec{E}_\theta = -V\vec{e}_R \times \vec{B}_z, \tag{8}$$

$$\frac{1}{\mu_0\varepsilon_0}\vec{B}_z = V\vec{e}_R \times \vec{E}_\theta. \tag{9}$$

Here, V denotes the propagation velocity of the electromagnetic field associated with the vacuum SW, and should also correspond to the velocity at which a charge or particle propagates the electromagnetic fields [10]. Given the absence of charges in a vacuum, V must therefore represent the magnitude of the absolute velocity of the propagation particle of the SWs $\vec{B}_z/\vec{E}_\theta$ relative to the vacuum medium.

The particle propagation mode for the vacuum SWs $\vec{B}_z/\vec{E}_\theta$ is illustrated in Fig. 1 [18]. To uphold the conservation of angular momentum within this model, it is hypothesized that the propagating particles of the SWs consist of two left-handed neutrinos undergoing counter-rotating large-helical revolution, with a phase difference of π. The spin velocity of the left-handed neutrinos equals the speed of light, and both follow left-handed large-helical trajectories along the forward axis, with their axial velocity V_z also matching the speed of light. Since neutrinos possess mass, their tangential rotational velocity V_θ cannot exceed the speed of light [32]. By assuming that the mechanism of neutrinos rotating around the SWs' core is analogous to that of a ground-state electron orbiting the hydrogen nucleus [33], we can derive

$$V_\theta = \frac{C}{137}. \tag{10}$$

From Ref. [10], the frequency of the helical motion of scalar wave neutrinos, denoted as ω_P, corresponds to the frequency of the vacuum SWs $\vec{B}_z/\vec{E}_\theta$ and can be expressed as

$$\omega_P = j\frac{1}{\tau_2} = j\frac{\omega^2\varepsilon_0}{\sigma_0} = 1.129 \times 10^{31}\ \text{Hz}. \tag{11}$$

Accordingly, the step length of the helical motion of their propagation particle (neutrino) can be expressed as

$$\lambda = C\tau_2 = 2.654 \times 10^{-25}\ \text{m}. \tag{12}$$

Herein, τ_2 denotes the vortex decay period of the vortex electric field $\vec{E}_\theta$, ω represents the frequency of the source light waves that generate the SWs, and σ_0 and ε_0 are the vacuum conductivity and vacuum permittivity, respectively.

Consequently, the energy ratio of $\vec{B}_z/\vec{E}_\theta$ to the source light waves can be expressed as

$$\frac{E_P}{E_T} = \frac{\hbar\omega_P}{\hbar\omega} = \frac{10^{31}\ \text{Hz}}{10^{13}\ \text{Hz}} = 10^{18}, \tag{13}$$

which implies that, in addition to the energy contribution E_T, the SWs $\vec{B}_z/\vec{E}_\theta$ must acquire a substantial amount of additional free energy from the zero-point vacuum field [10, 16]. The free energy acquisition mechanism of $\vec{B}_z/\vec{E}_\theta$ is associated with the local spatial vortex motions of the SW-propagating particles (neutrinos), where the vortex motion acts as the fundamental unit of energy and a bridge linking visible matter to invisible energy [18]. This vortex motion enables the extraction of zero-point vacuum energy via the coherent resonance effect between the torsion field they induce and the zero-point vacuum energy field [13, 14].

Given that SWs $\vec{B}_z/\vec{E}_\theta$ absorb a significant quantity of vacuum free energy, this energy—analogous to the local spatial curvature effect induced by massive objects and the gravitational field generated by spatial curvature—gives rise to a distinct spatial distortion effect within the helical interior of the SWs. This distortion manifests as a tangential distortion motion $V_{\theta 1}$ and a z-directional bending motion V_{z1} in the local space (see Fig. 2).

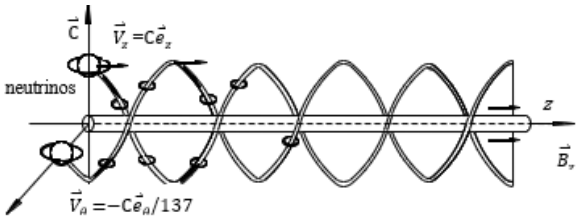

Figure 1. Particle propagation mode of vacuum SWs.

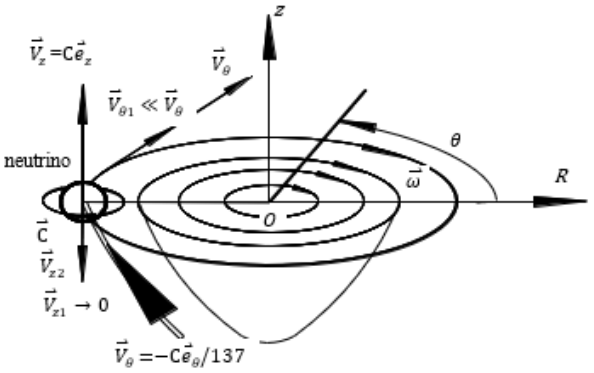

Figure 2. The helical motion of the neutrino around the core of the SWs.

To simplify the model, we assume the bending effect of the Earth in this local space corresponds to a z-directional bending motion V_{z2}, while neglecting the influence of macroscopic z-directional spatial expansion. Accordingly, the absolute equation of motion for the vacuum SW-propagating particle (neutrino) relative to the vacuum is expressed as

$$\vec{V} = C\vec{e}_z - \frac{C\vec{e}_\theta}{137} - V_{\theta 1}\vec{e}_\theta - V_{z2}\vec{e}_z. \tag{14}$$

Herein, $C\vec{e}_z$ denotes the linear motion of the SW neutrino at the speed of light along the z-direction, while $\frac{C\vec{e}_\theta}{137}$ corresponds to its tangential rotational motion. $V_{\theta 1}\vec{e}_\theta$ refers to the local spatial distortion motion induced by the scalar wave after it has absorbed a substantial amount of vacuum free energy, and $V_{z2}\vec{e}_z$ represents the z-direction bending motion of the Earth within this local space. Notably, $C\vec{e}_z$ and $\frac{C\vec{e}_\theta}{137}$ are the active motions of the scalar-wave neutrino, whereas $V_{z2}\vec{e}_z$ and $V_{\theta 1}\vec{e}_\theta$ are the passive motions of the SW neutrino that arise as a consequence of its following the spatial deformation.

4. The wave equations for SWs

As illustrated in Fig. 3, within the vacuum space, we establish a region **V** of the field point P centered at point O on the Earth's surface. In the source region **V′** (centered at the fixed source point O' adjacent to field region **V**), there exist certain continuous, non-moving, and time-varying charges $\rho(\vec{r}', t)$ and a time-varying vortex current source $\vec{J}_\theta(\vec{r}', t)$ that is excited by external electromagnetic fields. These sources generate the SWs $\vec{B}_z/\vec{E}_\theta$ within the region **V**.

Furthermore, a cylindrical coordinate system (R_1, θ, z) is established with an observer O_B as the origin on the Earth's surface. This coordinate system is employed to describe the propagation of the neutrino motion of $\vec{B}_z/\vec{E}_\theta$. When **V′** approaches zero and O_B coincides with O', the position vector $\vec{r}$ satisfies

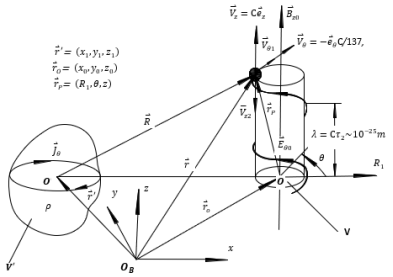

Figure 3. Distribution map of the source points and field points generating SWs in a vacuum.

$$\vec{r} = \vec{r}_P + \vec{r}_o \to \vec{R},$$

and

$$\begin{aligned}\frac{\partial R}{\partial t} = \frac{\partial r}{\partial t} = \frac{\partial r_P}{\partial t} &= \frac{\partial r_P}{\partial R_1}\frac{\partial R_1}{\partial t} + \frac{\partial r_P}{\partial \theta_1}\frac{\partial \theta_1}{\partial t} + \frac{\partial r_P}{\partial z}\frac{\partial z}{\partial t} \\ &= C - V_\theta - V_{\theta 1} - V_{z2}.\end{aligned} \tag{15}$$

Subsequently, in accordance with the relational formula between the scalar waves $\vec{B}_z/\vec{E}_\theta$ and $\vec{A}_\theta/\varphi_\theta$ [6], within region P, when the radial dimension $r = R = 10^{-3}\lambda \sim 10^{-28}$ m $\ll \lambda = C\tau_2 \sim 10^{-25}$ m and $V_{\theta 1} \ll C$:

$$\begin{aligned}\vec{B}_z = \nabla \times \vec{A}_\theta &= \frac{\mu_0}{4\pi}\int_{V'} \nabla \times \left(\frac{\vec{J}_\theta}{R}\right) dV' \\ &= \frac{\mu_0}{4\pi}\int_{V'} -R^{-2}\left(\vec{e}_R \times \vec{J}_\theta\right) dV' \\ &= \vec{e}_R \times \frac{\mu_0}{4\pi}\int_{V'} -R^{-2}\vec{J}_\theta dV',\end{aligned} \tag{16}$$

$$\begin{aligned}\vec{E}_\theta &= -\nabla\varphi_\theta - \frac{\partial \vec{A}_\theta}{\partial t} = -\frac{\partial \vec{A}_\theta}{\partial t} \\ &= \frac{\mu_0}{4\pi}\frac{\partial}{\partial t}\int_{V'}\left(\frac{\vec{J}_\theta}{R}\right) dV' \\ &= \frac{\mu_0}{4\pi}\frac{\partial R}{\partial t}\int_{V'} -R^{-2}\vec{J}_\theta dV' \\ &= (C - V_\theta - V_{\theta 1} - V_{z2})\,\vec{e}_R \times \vec{B}_z \\ &\approx C\vec{e}_R \times \vec{B}_z.\end{aligned} \tag{17}$$

From Eqs. (16) and (17), the fundamental equations for $\vec{B}_z/\vec{E}_\theta$ in a vacuum are derived as follows [6]:

$$\frac{1}{\mu_0\varepsilon_0}\nabla \times \vec{B}_z = \frac{\partial \vec{E}_\theta}{\partial t} = \frac{\vec{E}_\theta}{\tau_2}, \tag{18}$$

$$\nabla \times \vec{E}_\theta = -\frac{\partial \vec{B}_z}{\partial t} = -\frac{\vec{B}_z}{\tau_2}, \tag{19}$$

whose plane wave solutions are presented as Eqs. (20) and (20.1):

$$\vec{E}_\theta = CB_{z0}\exp\left[j\left(\frac{\omega_P}{C}z - \omega_P t\right)\right]\vec{e}_\theta, \tag{20}$$

$$\vec{B}_z = B_{z0}\exp\left[j\left(\frac{\omega_P}{C}z - \omega_P t\right)\right]\vec{e}_z. \tag{20.1}$$

Fig. 4 depicts the wave patterns of $\vec{E}_\theta$ and $\vec{B}_z$, showing that $\vec{E}_\theta$ and $\vec{B}_z$ share the same phase angle and propagate along the positive z-axis at the phase velocity C. Eqs. (20) and (20.1) unveil the electromagnetic induction law governing the vacuum SWs $\vec{E}_\theta$

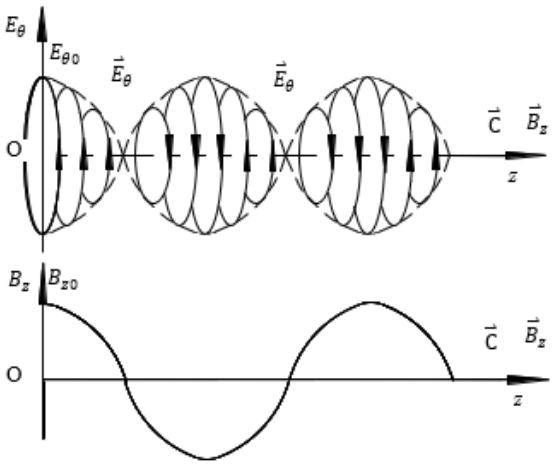

Figure 4. The wave propagation patterns of SWs $\vec{E}_\theta/\vec{B}_z$ in a vacuum.

and $\vec{B}_z$—specifically, the scalar magnetic field $\vec{B}_z$ and the vortex electric field $\vec{E}_\theta$ are mutually convertible and propagate forward in a vacuum.

Within the vacuum, the local spatial vortex motion induced by $\vec{E}_\theta$ interacts with the zero-point vacuum energy field, forming a torsion field coherence (resonance) state. This state generates high-energy rays, neutrons, and high-energy particles at the vortex center of the scalar wave, while extracting zero-point vacuum free energy—accompanied by highly directional cold nuclear fusion [13]. This process embodies the mechanism by which SWs harness free energy from the zero-point vacuum energy field.

5. Torsion fields induced by vacuum SWs

Upon differentiating the left-hand side of Eq. (17), we obtain

$$\frac{\partial \vec{E}_\theta}{\partial t} = \frac{\partial}{\partial t}\left(E_\theta \vec{e}_\theta\right) = \frac{E_\theta}{\tau_2}\vec{e}_\theta - \frac{E_\theta}{\tau_2}\vec{e}_R, \tag{21}$$

while upon differentiating the right-hand side of Eq. (17), we obtain

$$\begin{aligned}\frac{\partial \vec{E}_\theta}{\partial t} = C\vec{e}_R \times \frac{\vec{B}_z}{\tau_2} + C\vec{e}_\theta \times \frac{\vec{B}_z}{\tau_2} - V_\theta\vec{e}_\theta \times \frac{\vec{B}_z}{\tau_2} \\ - V_\theta\vec{e}_R \times \frac{\vec{B}_z}{\tau_2} - a_\theta\vec{e}_R \times \vec{B}_z - a_\theta\vec{e}_\theta \times \vec{B}_z \\ - g\vec{e}_R \times \vec{B}_z - g\vec{e}_\theta \times \vec{B}_z.\end{aligned} \tag{22}$$

In Eq. (22), $\frac{C}{\tau_2} \sim 10^{39}$ m/s^2 corresponds to the strong interaction scale. strong nuclear force field generated by the z-directional linear motion of the SW particle at the speed of light $C\vec{e}_z$, $\frac{V_\theta}{\tau_2} \sim 10^{37}$ m/s^2 undoubtedly represents the electromagnetic fields induced by its tangential subluminal rotational motion $V_\theta\vec{e}_\theta$, a_θ equaling $\frac{\partial V_{\theta 1}}{\partial t}$ denotes the acceleration field of the spatial tangential distortion motion induced by the vacuum SWs $\vec{B}_z/\vec{E}_\theta$ within their helical structure, namely the torsion field, and $g \sim 10$ m/s^2 denotes the gravitational field acting on the SW neutrino. Eq. (22) appears to formally unify nuclear force, electromagnetic force, torsion field force, and gravitational force [34, 35]. An analysis of Eq. (22) reveals that, under ideal conditions, SWs can generate a torsion field with a magnitude comparable to that of the strong nuclear force. However, in the field of medical therapy, SW torsion fields do not require such enormous energy; only the torsion field corresponding to the

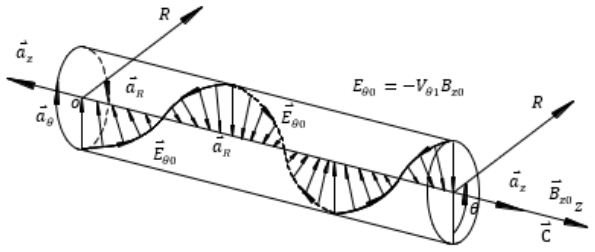

Figure 5. Artificial torsion fields generated by vacuum SWs.

local spatial tangential distortion motion $V_{\theta 1}$, induced by the vortex motion of SW particles, is necessary.

Based on Eqs. (21) and (22), when magnetism generates electricity, the electromagnetic fields adhere to the left-hand helix rule. The radial and tangential acceleration fields (i.e., the torsion fields $\vec{a}_R$ and $\vec{a}_\theta$) of the spatial tangential distortion motion $V_{\theta 1}\vec{e}_\theta$, induced by the vacuum SWs $\vec{B}_z/\vec{E}_\theta$, can be expressed as

$$\frac{E_\theta}{\tau_2}\vec{e}_\theta = -a_\theta \vec{e}_R \times \vec{B}_z, \tag{23}$$

$$\frac{E_\theta}{\tau_2}\vec{e}_R = a_\theta \vec{e}_\theta \times \vec{B}_z. \tag{24}$$

Meanwhile, based on Eq. (17), the electromagnetic conversion relation of the torsion-field-inducing SWs $\vec{B}_z/\vec{E}_\theta$ can be expressed as

$$\vec{E}_\theta = -V_{\theta 1}\vec{e}_R \times \vec{B}_z. \tag{25}$$

Projecting Eq. (25) onto the θ-direction as shown in Fig. 3 yields

$$-E_\theta = V_{\theta 1} \times B_z, \tag{26}$$

which indicates that the torsion-field-inducing SWs $\vec{B}_z/\vec{E}_\theta$ have a phase difference of 180°, i.e., $dE_\theta = -V_{\theta 1} dB_z$.

By combining Eqs. (23), (24), and (26), the torsion fields $\vec{a}_R$ and $\vec{a}_\theta$ generated by the vacuum SWs $\vec{B}_z/\vec{E}_\theta$ can be expressed as

$$\vec{a}_R = a_\theta \vec{e}_R = -\vec{E}_\theta \times \frac{\vec{B}_z}{B_z^2 \tau_2} = \frac{1}{B_z^2}\vec{B}_z \times \frac{\partial \vec{E}_\theta}{\partial t}, \tag{27}$$

$$\vec{a}_\theta = a_\theta \vec{e}_\theta = -\vec{e}_\theta \frac{V_{\theta 1}}{\tau_2} = -E_\theta \vec{e}_R \times \frac{\vec{B}_z}{B_z^2 \tau_2}. \tag{28}$$

Similarly, based on the relational Eqs. (16) and (17) between $\vec{B}_z/\vec{E}_\theta$ and $\vec{A}_\theta/\varphi_\theta$, when electricity generates magnetism, the electromagnetic conversion relation of the torsion-field-inducing SWs $\vec{B}_z/\vec{E}_\theta$ can also be expressed as $V_{\theta 1}^2 \vec{B}_z = V_{\theta 1}\vec{e}_R \times \vec{E}_\theta$.

Employing the same analytical approach, it is found that when electricity generates magnetism, the electromagnetic fields follow the right-hand helix rule. The z-directional acceleration field of the local spatial curvature motion induced by $\vec{B}_z/\vec{E}_\theta$—namely, the z-directional torsion field—can be expressed as

$$\vec{a}_z = a_\theta \vec{e}_z = \vec{e}_z \frac{V_{\theta 1}}{\tau_2} = \frac{\left(\vec{e}_R \times \vec{E}_\theta\right)}{B_z \tau_2}. \tag{29}$$

6. Dynamic analysis of thrombus removal induced by torsion fields

6.1. Negative mass induced by radial torsion field

According to the wave pattern of the vacuum SWs $\vec{B}_z/\vec{E}_\theta$ illustrated in Fig. 4, when magnetism induces electricity, the electromagnetic field follows the left-hand screw rule, and $\frac{\partial E_\theta}{\partial t} < 0$—meaning the vortex electric field E_θ decreases with time. Accordingly, the radial torsion field $\vec{a}_R$ associated with the spatial tangential distortion motion $V_{\theta 1}\vec{e}_\theta$ induced by $\vec{B}_z/\vec{E}_\theta$ can be expressed as

$$\vec{a}_R = a_\theta \vec{e}_R = -\frac{1}{B_z^2}\vec{B}_z \times \vec{e}_\theta \frac{\partial E_\theta}{\partial t} = -\frac{E_\theta}{B_z \tau_2}\vec{e}_R; \tag{30}$$

when electricity induces magnetism, the electromagnetic field obeys the right-hand screw rule, and $\frac{\partial E_\theta}{\partial t} > 0$—meaning the vortex electric field E_θ increases with time. Accordingly, the radial torsion field $\vec{a}_R$ associated with the spatial tangential distortion motion $V_{\theta 1}\vec{e}_\theta$ induced by $\vec{B}_z/\vec{E}_\theta$ can be expressed as

$$\vec{a}_R = a_\theta \vec{e}_R = \frac{1}{B_z^2}\vec{B}_z \times \vec{e}_\theta \frac{\partial E_\theta}{\partial t} = -\frac{E_\theta}{B_z \tau_2}\vec{e}_R. \tag{31}$$

It is evident that regardless of whether electricity induces magnetism or magnetism induces electricity, the direction of the radial torsion field $\vec{a}_R$ generated by $\vec{B}_z/\vec{E}_\theta$ is as illustrated in Fig. 5: the radial torsion field $\vec{a}_R$ is an intense spiral centripetal acceleration field.

With reference to the definitions of relevant physical quantities in electrostatic fields [36], within a stationary spherical space **R**, we define the gravitational field $\vec{a}$, gravitational potential φ_g, gravitational displacement vector $\vec{F}$, and global gravitational flux ϕ_g induced by a spherical object of mass M located at the space center O (with radius r_0, density ρ, surface area S, and volume V, respectively) as follows (see Fig. 6):

$$\vec{a} = -\frac{GM}{r^2}\vec{e}_R \tag{31.1}$$

$$\varphi_g = \frac{-GM}{r}, \tag{31.2}$$

$$\vec{F} = \frac{1}{4\pi G}\vec{a} = -\frac{M}{4\pi r^2}\vec{e}_R, \tag{31.3}$$

$$\phi_g = \oint_S -\vec{F} \cdot d\vec{S} = \oint_S -\frac{1}{4\pi G}\vec{a} \cdot d\vec{S} = \frac{M}{4\pi}\oint_S \frac{1}{r^2} dS = M. \tag{31.4}$$

Herein, G denotes the gravitational constant, and r is the radial distance from the center O of the spherical space **R**. Eq. (31.4) implies that the essence of mass M lies in the total surface integral of the gravitational field $\vec{a}$ induced by it (i.e., the gravitational flux). Taking the cylindrical surface formed by the helical motion of SW neutrinos in Fig. 5 as the Gaussian surface, and assuming that the lateral surface area of this Gaussian surface is much larger than the area of its two end faces, the total Gaussian surface integral of the torsion field $\vec{a}_R$ induced by $\vec{B}_z/\vec{E}_\theta$ can be expressed as

$$\oint_S -\frac{1}{4\pi G}\vec{a}_R \cdot d\vec{S} = \oint_S -\frac{1}{4\pi G}\frac{V_{\theta 1}}{r^2 \tau_2} dS = -\frac{1}{4\pi G}\frac{V_{\theta 1}}{r^2 \tau_2} 2\pi RL = -M. \tag{31.5}$$

Herein, L denotes the thrombus length and $R$$denotesitsradius.WhentheSWt
is responsible for the mass reduction of the thrombus. Once the thrombus mass is reduced to zero, it enters a wave state and exits the human body at the speed of light. Concurrently, as the thrombus transitions into the wave state, the medical treatment mechanisms and approaches for cardiovascular and cerebrovascular thrombosis may undergo qualitative changes.

6.2. Coagulation motion of thrombus induced by tangential torsion field

It is evident that regardless of electromagnetic induction (whether electric fields generate magnetic fields or vice versa), the direction

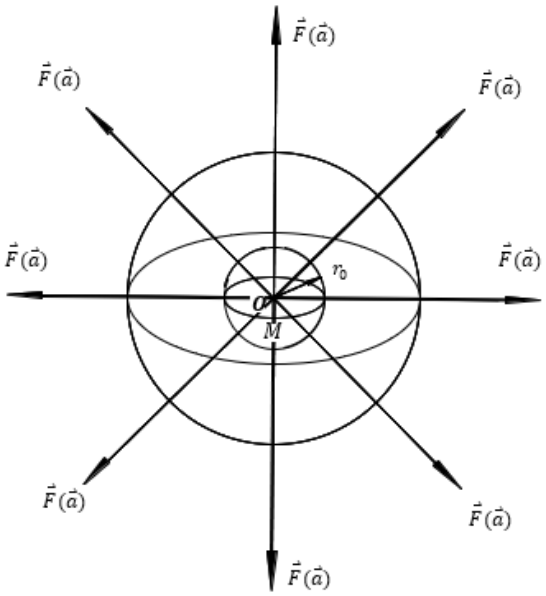

Figure 6. Gravitational field and displacement vector produced by a mass M.

of the tangential torsion field $\vec{a}_\theta$ induced by $\vec{B}_z/\vec{E}_\theta$ is illustrated in Fig. 5: the tangential torsion field $\vec{a}_\theta$ causes local space to rotate clockwise (when viewed from the positive to the negative direction of $\vec{B}_z$). Analogous to centrifugation techniques, $\vec{a}_\theta$ promotes the aggregation of thrombogenic factors derived from positively charged dysfunctional red blood cells in human blood, forming helical filamentous thrombus clusters. This process reduces thrombus volume and mitigates the challenges associated with thrombus management.

6.3. Directional guidance of thrombus removal by z-axis torsion field

According to Eq. (29), the z-directional bending acceleration field induced by the local spatial distortion motion triggered by $\vec{B}_z/\vec{E}_\theta$, namely the z-directional torsion field $\vec{a}_z$, can be expressed as

$$\begin{aligned}\vec{a}_z = a_\theta \vec{e}_z = \vec{e}_z \frac{V_{\theta 1}}{\tau_2} = \frac{\left(\vec{e}_R \times \vec{E}_\theta\right)}{B_z \tau_2} \\ = \frac{1}{B_z}\left(\vec{e}_R \times \frac{\partial \vec{E}_\theta}{\partial t}\right).\end{aligned} \tag{32}$$

As electricity induces magnetism, $\frac{\partial E_\theta}{\partial t} > 0$, meaning the vortex electric field E_θ increases with time,

$$\vec{a}_z = a_\theta \vec{e}_z = \frac{1}{B_z}\left(\vec{e}_R \times \frac{\partial E_\theta}{\partial t}\vec{e}_\theta\right) = \vec{e}_z \frac{V_{\theta 1}}{\tau_2}; \tag{33}$$

while as magnetism induces electricity, $\frac{\partial E_\theta}{\partial t} < 0$, meaning the vortex electric field E_θ decreases with time,

$$\vec{a}_z = a_\theta \vec{e}_z = \frac{1}{B_z}\left(\vec{e}_R \times \frac{\partial E_\theta}{\partial t}\vec{e}_\theta\right) = -\vec{e}_z \frac{V_{\theta 1}}{\tau_2}. \tag{34}$$

It is evident that the expression of the z-directional torsion field $\vec{a}_z$ induced by SWs $\vec{B}_z/\vec{E}_\theta$ still adheres to Newton's laws of motion. Its direction is either consistent with or opposite to the propagation direction of the scalar magnetic field $\vec{B}_z$ of the scalar wave, depending on the rate of change of the vortex electromagnetic field E_θ. When the SW torsion fields target cardiovascular and cerebrovascular thrombi, the dominant motion of the thrombus driven by the z-directional torsion field $\vec{a}_z$ governs the direction of thrombus removal.

7. The interaction between vacuum SWs and red blood cells

The primary component of blood consists of red blood cells, and thrombus formation essentially arises from the adhesion of red blood cells. The surface of each healthy red blood cell carries a negative charge. With aging and the occurrence of metabolic abnormalities, the surface of pathological red blood cells becomes enveloped by a lipid membrane, which diminishes or abolishes their negative surface charge while augmenting the positive charge. This leads to electrostatic attraction between pathological and healthy red blood cells, culminating in the formation of what is known as a thrombus.

Mature red blood cells shed their nuclei and mitochondria to maximize the spatial capacity for hemoglobin, thereby optimizing their oxygen-transport function. They rely on anaerobic glycolysis to generate adenosine triphosphate (ATP) for energy supply. ATP is indispensable for all life processes. Fluctuations in the ATP/adenosine diphosphate (ADP) ratio are intricately linked to numerous pathways, including apoptosis, autophagy, and energy metabolism, and thus ATP/ADP ratio is frequently employed as one of the indicators for assessing cell viability[38]. When ATP is hydrolyzed into ADP and inorganic phosphate, energy is released to drive a multitude of intracellular biochemical processes, which in turn stimulates, balances, and enhances the energy of the organism's biological field, facilitating the restoration of health.

In the process of blood circulation, the most fundamental chemical reaction is electron transfer, which is mediated by hemoglobin. Hemoglobin molecules are, in fact, long chains formed by the linkage of amino acid molecules, each exhibiting identical left-handed chirality.

When a living organism receives the left-handed SW (carrying drug/nutrient information and zero-point vacuum energy) emitted by a SW generator, the scalar magnetic field B_L of the left-handed SW induces a left-handed eddy potential $\vec{E}_v$ channel along hemoglobin molecular chain (see Fig. 7) while delivering information and energy to cells. This left-handed $\vec{E}_v$ attracts left-spinning free electrons in the cell fluid to move left-handedly along hemoglobin chains, accelerating the dissociation of intracellular water molecules into H^+ and OH^- (the source of free electrons). This disrupts the intracellular ATP/ADP concentration balance, thereby accelerating the synthesis of ATP from ADP and inorganic phosphate, and decelerating ATP hydrolysis. The release of free electrons also stimulates the antioxidant activity of cells, increasing the ATP/ADP concentration ratio in red blood cells, promoting blood circulation, and maintaining the organism in a high-energy state (see Fig. 7).

When cells interact with the scalar magnetic field B_R of right-handed SWs, the organism generates B_R at the center of hemoglobin chains. The device regulates B_R to induce a right-handed $\vec{E}_v$ channel, which repels free electrons in the cell fluid. This accelerates the recombination of H^+ and OH^- into water molecules, thereby accelerating ATP hydrolysis into ADP and inorganic phosphate in red blood cells, while decelerating ATP synthesis. The ATP/ADP ratio in red blood cells decreases, blood circulation slows, and the organism enters a low-energy state.

The energy required for ATP synthesis is derived from three sources: food oxidation (in animal cells, fungi, and some bacteria), light energy capture (in plant cells and some bacteria), and zero-point

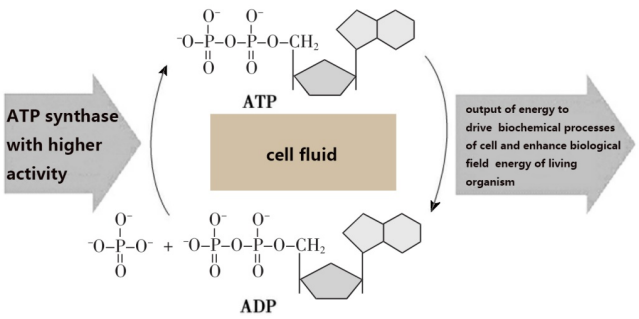

Figure 7. ATP/ADP mutual conversion in mitochondria of cells under the action of SWs.

vacuum energy supplied by scalar waves (applicable to both animal and plant cells).

From the above analysis, SWs are closely associated with normal blood circulation and thrombus formation. The quantity of free electrons provided by SWs not only directly determines thrombus size and concentration but also regulates the ATP/ADP ratio in red blood cells. Left-handed SWs supply free electrons to red blood cells, increasing their ATP/ADP ratio, accelerating blood circulation, and sustaining the organism in a high-energy state.

8. Conclusion

Based on the rigorous vacuum SW equations and particle propagation mode, we propose a theoretical model for the torsion fields generated by vacuum SWs, revealing their intrinsic connections to mass and gravitational field. The establishment of these novel torsion field theoretical models provides feasible solutions to bottleneck issues in the research on medical applications of torsion fields—such as the optimization of torsion field energy intensity and SW therapeutic frequency—while offering new tools and implementation approaches for analyzing the medical functions and physicochemical mechanisms of torsion fields generated by vacuum SWs in the treatment of cardiovascular and cerebrovascular diseases. Finally, we conduct a detailed analysis of the dynamic characteristics of thrombus removal by the torsion fields and the interaction between SWs and red blood cells.

The magnitude of the torsion field generated by vacuum SWs is correlated with the variation frequency and electromagnetic conversion efficiency of the SW electromagnetic field, i.e., the velocity of local spatial distortion motion induced by SWs within the helix. The theoretical expression of the torsion field generated by SWs still adheres to Newton's laws of motion: the direction of the z-axis torsion field is either parallel or antiparallel to the propagation direction of the SW, depending on the rate of change of the scalar electric field E_z, which dictates the direction of thrombus removal; the radial torsion field is a strong helical centripetal acceleration field that induces the mass-reduction process of thrombi; the tangential torsion field drives the rotation of local space inside the SW helix, leading to thrombus aggregation. The three torsion fields act as a precise micro-surgical scalpel, enabling non-invasive aggregation and removal of intravascular thrombi while delivering energy and information to living organisms and enhancing their bioenergetic fields.

ACKNOWLEDGEMENTS

I would like to thank my wife, Ms. Xue Jingwen for her hard family work and support for my creation of this thesis.

COMPETING INTERESTS

The authors declare no competing interests.

DATA AND MATERIALS AVAILABILITY

All data are available in the main text or the supplementary materials.

ETHICS DECLARATIONS

The study did not require ethical approval.

APPROVAL FOR ANIMAL EXPERIMENTS

Confirms that all experiments were performed in accordance with relevant named guidelines and regulations.

APPROVAL FOR HUMAN EXPERIMENTS

Confirms that all experiments were performed in accordance with relevant named guidelines and regulations.

REFERENCES

[1] Shahneh A, et al. Impact of pulsed electromagnetic field therapy on vascular function and blood pressure in hypertensive individuals[J]. *Hypertension Research*, 2021, 44(9):1185-1192. https://doi.org/10.1038/s41440-021-00734-7.

[2] Zeng Y, et al. Pulsed electromagnetic field improves cardiac function in response to myocardial infarction[J]. *Scientific Reports*, 2019, 9(1):1-12. https://doi.org/10.1038/s41598-019-45939-5.

[3] Hu Tao, Lü Anlin, Zhang Rongqing, et al. Effects of low-frequency electromagnetic fields on nitric oxide synthase in cultured human umbilical vein endothelial cells [J]. *Chinese Journal of Physical Medicine & Rehabilitation*, 2001. DOI: CNKI:SUN:ZHLY.0.2001-05-012.

[4] Zhang Y, et al. Electromagnetic field and cardiovascular diseases: A state-of-the-art review of diagnostic, therapeutic, and predictive values[J]. *FASEB BioAdvances*, 2023, 5(8):vbac167. https://doi.org/10.1096/fba.2023-00167.

[5] Jafari R, et al. Electromagnetic field therapy in cardiovascular diseases: A review of patents, clinically effective devices, and mechanism of therapeutic effects[J]. *Trends in Cardiovascular Medicine*, 2021, 33(2):72-78. https://doi.org/10.1016/j.tcm.2021.10.006.

[6] Jiang, J. Z., and Wang, Y. F. 2024. Analysis of the Electromagnetic Characteristics and the Mechanism Underlying Bio-Medical Function of Longitudinal Electromagnetic (LEM) Waves. *J. Energy and Power Engineering* 12 (10): 31-49.

[7] Cessenat M. *Mathematical Methods in Electromagnetism*[M]. Singapore: World Scientific, 1996.

[8] Carbajal-Domínguez A, et al. Numerical calculation of near field scalar diffraction using angular spectrum of plane waves theory and FFT[J]. *arXiv preprint arXiv:2304.02653*, 2023.

[9] Oschman J. *Energy Medicine: The Scientific Basis*[M]. Edinburgh: Elsevier Science, 2000, 203-206.

[10] Jiang, J. Z., and Wang, Y. F. 2024. The Magnetic Longitudinal (P-) Wave's Propagation and Energy Models Underlying the Mechanisms of Its Capacity to Absorb Free Energy. *J. Energy and Power Engineering* 12 (7): 39-62.

[11] Akimov AE, Tarasenko VY. Models of polarized states of the physical vacuum and torsion fields. *Izvestiya Vysshikh Uchebnykh Zavedenii Fizika*. 1992;35(3):13-23.

[12] Lee, S. C. 2020. *The Science of Torsion Field.* Taipei: Sancai Culture Publishing Co., Ltd.

[13] Jiang X L, Lei J.Z., Han L.J. Torsion field and tapping the zero-point energy in an electrochemical system[J]. *J. of New Energy*, 1999, 4(2):93.

[14] Lei Jinzhi, Jiang Xingliu, Zhang Jiangang, et al. Electrochemical Anomalous Phenomena and Torsion Field Theory [J]. *Science & Technology Review*, 2000, (6): 3. DOI: 10.3321/j.issn:1000-7857.2000.06.001.

[15] Liang W C, Lee S C. Velocity, gyroscopic procession, and spin-curvature force[J]. *Phys. Rev. D*, 2013, 87(4): 044024.

[16] Don R. Excitation and extraction of vacuum energy via EM-torsion field coupling theoretical model[J]. *J. New Energy*, 1998, 3 (2/3), 130-131.

[17] Akimov AE, Tarasenko VY, Shipov GI. Torsion fields as a cosmophysical factor. *Biofizika*. 1995;40(4):938.

[18] Jiang Xingliu. The 21st Century Is the Century of Zero-Point Energy [J]. *Frontiers of Science*, 2010. DOI: CNKI:SUN:QYKX.0.2010-03-005.

[19] Ebbers J A, Meyl K. Drug effects in yeast mediated by scalar waves[J]. *Med. Sci.*, 2014, 8: 58-62.

[20] Rein G. Biological Interactions with Scalar Energy-Cellular Mechanisms of Actions[C]. *Proceedings Seventh International Association Psychotronics Research*. Georgia: December, 1988.

[21] Meyl K. Magnetic Wave Transmission of Drug Effects about the Waves, Generated in the Measurement Set-Up and Used i.e. for Anticancer-Treatments[J]. *Journal of US-China Medical Science*, 2019, 16:134-139.

[22] H. Schnabl, K. Meyl. Longitudinal magnetic waves trigger higher ATP-levels and extend the aging process of plants[J]. *Biol. Eng. Med.* 2018, 3: 1-4.

[23] H. Schnabl, K. Meyl. Anti-Aging by longitudinal magnetic waves: A new approach by modulating ATP-Levels[J]. *Biol. Eng. Med.* 2019, 4:1-5. DOI 10.15761/BEM.1000175.

[24] Meyl, K. 1998 Teil 1: Umdruck zur Vorlesung. Villingen-Schwenningen. 3. Auflage, 75-79.

[25] Zohuri B, Masoud J M. Longitudinal Scalar Wave (LSW) Fact: It Is a True Science, Neither Pseudoscience Nor Fiction (A Short Memorandum) [J]. *Journal of Energy and Power Engineering*, 2023, 17: 57-62.

[26] Guo S H (revised by Huang N B, Li Z B, Lin Q G) 2008 *Electrodynamics* (3rd.) (Beijing: China: Higher Education Press) pp121-158.

[27] Chen Youjun. The Moving Electric Field Possesses Magnetic Field Characteristics: The Relationship between Electric Field and Magnetic Field (2) [J]. *Journal of Inner Mongolia Agricultural University: Natural Science Edition*, 2002, 23(1):7. DOI: 10.3969/j.issn:1009-3575.2002.01.020.

[28] Chen Youjun. The Moving Magnetic Field Has the Characteristics of an Electric Field - One of the Electromagnetic Relationships [J]. *Journal of Inner Mongolia Agricultural University: Natural Science Edition*, 2001, 22(4):7. DOI: 10.3969/j.issn:1009-3575.2001.04.024.

[29] Jiang Jian-zhong. A mode of electromagnetic wave propagation based on the inter-induction of scalar electric field and vortex magnetic field. *Journal of Environmental Science and Engineering B* 13 (2024) 134-143. doi: 10.17265/2162-5263/2024.04.002.

[30] Huang K. *Solid state physics* (China: Higher Education Press, Beijing) 1998.

[31] Y. Aharonov, D. Bohm. Significance of electromagnetic potentials in the quantum theory. *Phys. Rev.* 115, 485–491(1959). DOI 10.1103/PhysRev.115.485 (1959).

[32] JIANG Jian-zhong, Chen Xi-Qi. An analysis about the origin and essence of mass based on particle-propagating model and wave equations of scalar waves. *Journal of Environmental Science and Engineering B* 14 (2025) 65-75 doi: 10.17265/2162-5263/2025.02.003.

[33] Bohr N. On the Constitution of Atoms and Molecules. *Phil. Mag.* 26 (1913)1.

[34] J. Z. Jiang, X. Q. Zhang. Unified Field Equation Generated by Longitudinal Electromagnetic (LEM) Waves. *Journal of Environmental Science and Engineering B* 13 (2024) 181-191. doi: 10.17265/2162-5263/2024.05.002.

[35] JIANG Jian-zhong, Chen Xi-Qi. An analysis about the origin and essence of mass based on particle-propagating model and wave equations of scalar waves. *Journal of Environmental Science and Engineering B* 14 (2025) 65-75 doi: 10.17265/2162-5263/2025.02.003.

[36] Jiang, J. and Zhang, X. (2025) The Relationship between the Gravitational Field and the Speed of Light. *Journal of Power and Energy Engineering*, 2025, 13(11), 1-12. doi: 10.4236/jpee.2025.1311001.